Dalton Transactions

Cite this: *Dalton Trans.*, 2011, **40**, 6691

www.rsc.org/dalton

PAPER

Synthesis and structure of tridentate bis(phosphinic amide)-phosphine oxide complexes of yttrium nitrate. Applications of ^{31}P,^{89}Y NMR methods in structural elucidation in solution†

Cristinel Popovici,[a] Ignacio Fernández,[a] Pascual Oña-Burgos,[a] Laura Roces,[b] Santiago García-Granda[b] and Fernando López Ortiz*[a]

Received 3rd February 2011, Accepted 11th April 2011
DOI: 10.1039/c1dt10194c

The synthesis and characterisation of a tridentate ligand containing two diphenylphosphinic amide side-arms connected through the *ortho* position to a phenylphosphine oxide moiety and the 1 : 1 and 2 : 1 complexes formed with yttrium nitrate are reported for the first time. The free ligand (R_{P1}*,S_{P3}*)-**11** is obtained diastereoselectively by reaction of *ortho*-lithiated *N*,*N*-diisopropyl-*P*,*P*-diphenylphosphinic amide with phenylphosphonic dichloride. Complexes [Y((R_{P1}*,S_{P3}*)-**11**)$(NO_3)_3$] and [Y((R_{P1}*,S_{P3}*)-**11**)$_2(NO_3)$][$(NO_3)_2$ were isolated by mixing ligand **11** with $Y(NO_3)_3{\cdot}6H_2O$ in acetonitrile at room temperature in a ligand to metal molar ratio of 1 : 1 and 2 : 1, respectively. The 1 : 1 derivative is the product of thermodynamic control when a molar ratio of ligand to yttrium salt of 1 : 1 is used. The new compounds have been characterised both as the solid (X-ray diffraction) and in solution (multinuclear magnetic resonance). In both yttrium complexes the ligand acts as a tridentate chelate. The arrangement of the two ligands in the 2 : 1 complex affords a pseudo-*meso* structure. Tridentate chelation of yttrium(III) in both complexes is retained in solution as evidenced by ^{89}Y NMR data obtained *via* ^{31}P,^{89}Y-HMQC, and ^{89}Y,^{31}P-DEPT experiments. The investigation of the solution behaviour of the Y(III) complexes through PGSE NMR diffusion measurements showed that average structures in agreement with the 1 : 1 and 1 : 2 stoichiometries are retained in acetonitrile.

Introduction

Reprocessing of spent nuclear fuels is based on the separation of the different radioactive components obtained by dissolution of the irradiated material in nitric acid. A critical aspect of the process is the efficient separation of lanthanides from actinides. This task is mostly achieved *via* liquid–liquid extraction procedures.[1] Extractants containing strong oxygen donor centers are particularly attractive for binding to the oxophilic trivalent f-element ions. In this context, phosphine oxides and carboxamides are among the preferred functional groups used to form coordination complexes with lanthanides and actinides. The studies have shown that polyfunctional ligands are superior extractants in comparison to monofunctional molecules.[2] For instance, carbamoylphosphine oxides (CMPOs, **1**, Fig. 1) are used in the TRUEX (**TR**ans**U**ranium **EX**traction) process and other variants[3] to coextract trivalent lanthanide and actinide ions remaining in the waste liquid resulting from the application of the PUREX (**P**lutonium **UR**anium **EX**traction using tri-*n*-butyl phosphate, TBP, **2**, Fig. 1) method.[4] The better extracting efficiency of CMPOs is derived from the presence of the P═O and C(═O)N linkages in the same molecule.

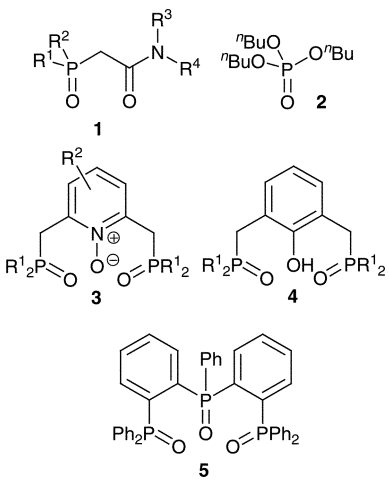

Fig. 1 Examples of PO-based ligand architectures used in the complexation of trivalent lanthanide ions.

[a]*Área de Química Orgánica, Universidad de Almería, Carretera de Sacramento, 04120, Almería. E-mail: flortiz@ual.es; Fax: +34 950 015481; Tel: +34 950 015478*
[b]*Departamento de Química Física y Analítica, Universidad de Oviedo-CINN, C/Julián Clavería 8, 33006, Oviedo, Spain*

† CCDC reference numbers 806039 (R*$_{P1}$,S_{P3}*)-**11**, 806041 [Y((R_{P1}*,S_{P3}*)-**11**)$(NO_3)_2$] and 806040 [Y((R_{P1}*,S_{P3}*)-**11**)$_2(NO_3)$][$(NO_3)_2$. For crystallographic data in CIF or other electronic format see DOI: 10.1039/c1dt10194c

It has been found that phosphine oxides interact with lanthanide cations more strongly than amides.[5] As a result, one may expect that replacing the C═O group of carboxamides by a P═O moiety would lead to ligands with enhanced ability for binding to f-block ions. The coordination of simple phosphine oxides[6] and multifunctional[7] PO-based ligands with lanthanide salts has been extensively investigated. Representative examples of tridentate molecules **3**,[8] **4**[9] and **5**[10] related to the title compound are given in Fig. 1. In the same vein, adducts formed between various lanthanide salts and a series of diphenylphosphinamides ($Ph_2P(O)NR^1R^2$, $R^1 = R^2 = H$,[11] Me,[12] $R^1R^2 = (CH_2CH_2)_2O$,[13] $R^1 = H$, $R^2 = Et$[14]) have been examined, although only in a few cases structural data at a molecular level have been reported.[15] The group 3 metal yttrium exhibit similar chemical behavior as the lanthanide elements.[16,11,12,13] Yttrium(III) shows an ionic radius intermediate between that of Dy^{3+} and Ho^{3+} and is often treated as part of the rare earth metals group. Contrary to most trivalent lanthanide ions, complexes of Y^{3+} are diamagnetic. Moreover, the ^{89}Y nucleus is a monoisotopic species of spin $I = \frac{1}{2}$ amenable to obtaining high resolution ^{89}Y-NMR spectra. These features allow the use of Y^{3+} complexes as models for investigating the solution behavior of structurally related paramagnetic complexes of lanthanides including extraction properties.[17]

We have previously shown that diphenylphosphinamides **6** can be efficiently deprotonated at the *ortho* position and the anions obtained act as C–C–P–O pincer ligands in the formation of five-membered ring metalocycles of lithium, **7**,[18] tin(IV), **8**, and gold(III),[19] **9**, or in the preparation of β-phosphine–phosphinamide bidentate ligands **10** (Fig. 2).[20] We reasoned that the same methodology could be readily extended to the preparation of a new family of phosphine oxide–phosphinamide tridentate ligands such as **11** (Fig. 2) that could bind to oxophilic cations through the three P═O groups of the molecule. Here we report: 1) the synthesis of *meso*-**11**, 2) the coordination complexes formed with yttrium nitrate using 1 : 1 and 2 : 1 molar ratios of ligand to yttrium salt, and 3) the structural characterisation of all new products in the solid-state and in solution through multinuclear magnetic resonance (^1H, ^{13}C, ^{31}P, ^{89}Y) techniques. ^{89}Y NMR data derived from experiments based on the existence of $^{89}Y,^{31}P$ coupling constants ($^{31}P,^{89}Y$-HMQC, and $^{89}Y,^{31}P$-DEPT) together with PGSE NMR diffusion studies allowed to identify the structure of the species present in solution.

Results and discussion

Synthesis of yttrium complexes

Ligand **11** was readily synthesized *via ortho* deprotonation of phosphinic amide **6** with the complex [*n*-BuLi·TMEDA] in toluene at –90 °C.[19a,20] The reaction of the *ortho* anion thus generated with 0.5 equiv of $PhP(O)Cl_2$ leads to the diastereoselective formation of **11** in an isolated yield of 55% (Scheme 1, reaction 1).

The molecule (R_{P1}*,S_{P3}*)-**11** is a *meso* compound containing two *ortho*-substituted phosphinic amide fragments bridged by a central phosphine oxide core which form a pocket of three P═O groups suitable for binding to oxophilic metals. The reaction of $Y(NO_3)_3{\cdot}6H_2O$ with (R_{P1}*,S_{P3}*)-**11** in a 1 : 1 molar ratio in acetonitrile solution during 4 h afforded a mixture of two complexes as evidenced by the ^{31}P NMR spectrum (Scheme 1, reaction 2). Two sets of signals were identified with the aid of a phase-sensitive ^{31}P COSY 2D experiment (Fig. 3) and assigned to complexes **12** (δ_P 33.4, 36.0, and 42.7 ppm) and **13** (δ_P 34.3, 40.3, and 42.0 ppm). Interestingly, the most deshielded signal of each complex showed cross-peaks with two ^{31}P signals. This pattern of correlations allows assignment of the signals at δ_P 42.7 and 42.0 ppm to the central phosphine oxide groups of complex **12** and **13**, respectively. The existence of two correlations for these P═O signals implies that complexation of (R_{P1}*,S_{P3}*)-**11** to yttrium is accompanied by the lost of symmetry of the ligand.

^{31}P NMR monitoring of this reaction at ambient temperature showed that the group of signals attributed to complex **12** increased with increasing reaction time, which also produced the progressive diminution of the relative concentration of complex **13** (Fig. 4). Quantitative conversion to complex **12** was achieved after 4 days under these conditions. These findings support the existence of a thermodynamic equilibrium between complexes **12** and **13**, with the former being the most stable species for the stoichiometry employed.

When the reaction between ligand (R_{P1}*,S_{P3}*)-**11** and $Y(NO_3)_3{\cdot}6H_2O$ was performed using a 2 : 1 molar ratio complex **13** was obtained in a few minutes in quantitative yields (Scheme 1, reaction 3). Furthermore, the formation of the 2 : 1 complex is diastereospecific. The relative face-to-face binding of the two tridentate ligands to the cation could afford two diastereoisomers corresponding to compounds with a *syn* arrangement of the phosphinic amide centers of the same or opposite chirality.

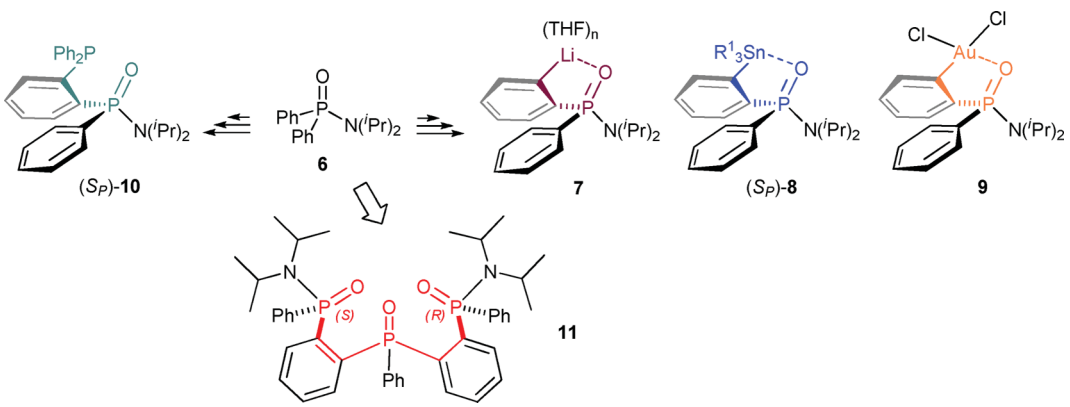

Fig. 2 Chelating ligands and complexes derived from *ortho* functionalized *P*,*P*-diphenylphosphinic amides.

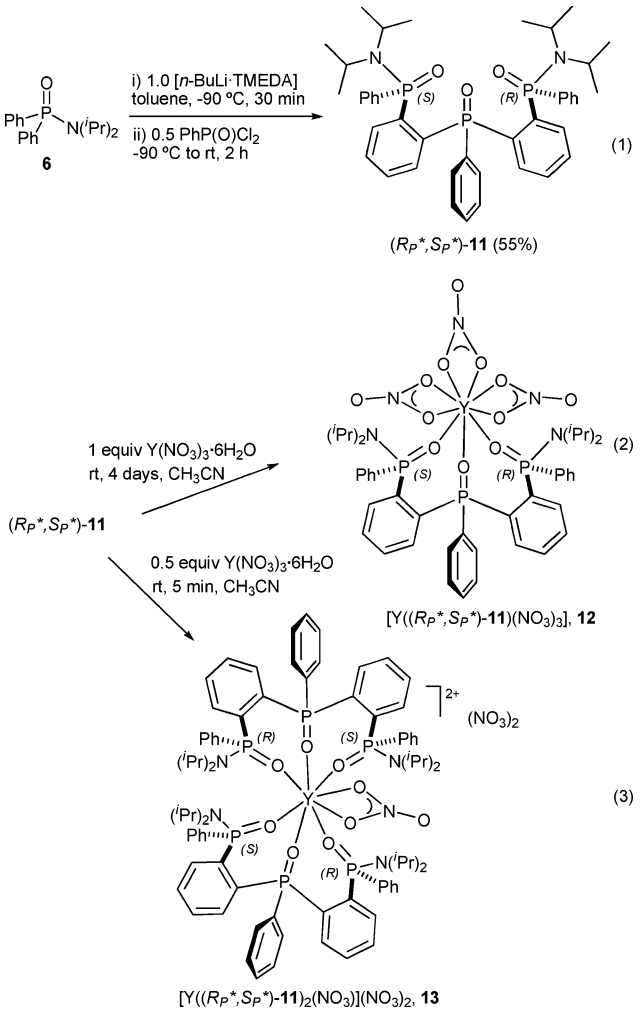

Scheme 1 Reaction schemes for (1) the diastereoselective synthesis of the tridentate bis(phosphinic amide)-phosphine oxide ligand (R_{P1}*,S_{P3}*)-**11**, (2) synthesis of complex [Y((R_{P1}*,S_{P3}*)-**11**)$(NO_3)_3$], **12**, and (3) synthesis of complex [Y((R_{P1}*,S_{P3}*)-**11**)$_2(NO_3)$]$(NO_3)_2$, **13**.

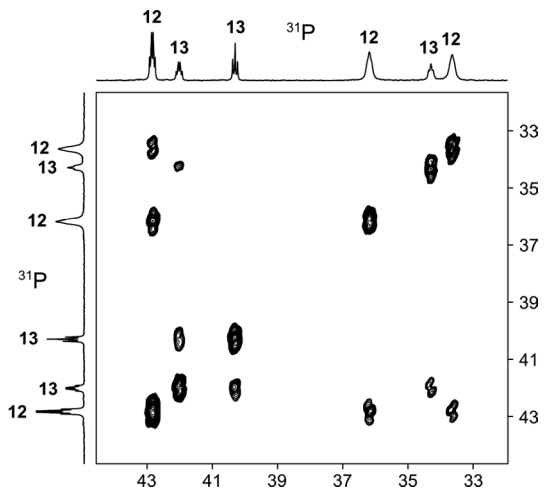

Fig. 3 2D ^{31}P COSY (121.49 MHz) of the reaction crude resulting from the equimolecular mixture of (R_{P1}*,S_{P3}*)-**11** and $Y(NO_3)_3·6H_2O$ in CD_3CN at room temperature after 30 min of reaction.

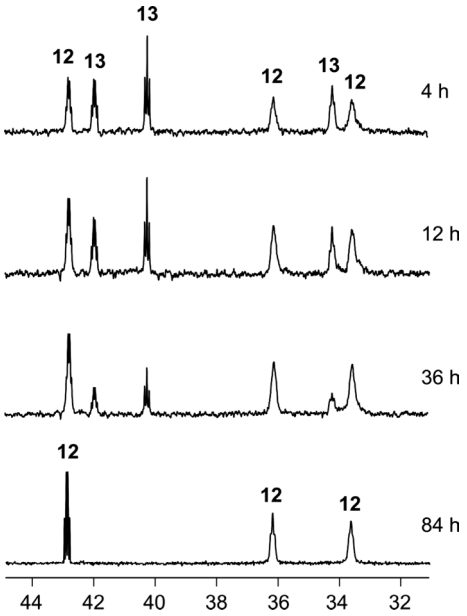

Fig. 4 ^{31}P NMR (121.49 MHz) monitoring of the reaction of equimolar amounts of (R_{P1}*,S_{P3}*)-**11** and $Y(NO_3)_3·6H_2O$ in CD_3CN at room temperature. NMR spectra acquired at reaction times of 4, 12, 36, and 84 h.

Complex **13** proved to be stable in acetonitrile solution over several weeks without any sign of decomposition. Moreover, for ligand : yttrium stoichiometries greater than 2 : 1, *i.e.* 3 : 1 or 4 : 1, the ^{31}P NMR spectra showed the coexistence of complex **13** and free ligand in agreement with an stable complex not prone to dissociate and/or aggregate (see diffusion NMR studies). The preference for the formation of the 2 : 1 complex **13** with respect to the 1 : 1 species **12** is somewhat surprising[8d,e,9a] due to intraligand interactions.[5d,e] However, this behavior is precedented in the lanthanide literature.[8c,21]

Solid state characterisations

Solid state structural characterisation of the new compounds synthesized was achieved by single crystal X-ray diffraction analysis. Crystals of (R_{P1}*,S_{P3}*)-**11** were grown by layering diethyl ether over a concentrated chloroform solution of **11**. The molecular structure is shown in Fig. 5, and allows the unequivocal assignment of the relative stereochemistry of the chiral phosphorus atoms as (R_{P1}*,S_{P3}*), *i.e.*, the optically inactive *meso* form. Selected data are summarized in Tables 1 and 2. The molecule may be described as a triphenylphosphine oxide derivative with two *P*-phenyl rings bearing a phenylphosphinic amide *ortho* substituent. The *ortho* substituted rings adopt a quasi-perpendicular arrangement (torsion angle C1–C2–P2–C19 of 165.1(2)°) that places the three phosphorus atoms in a plane and one phosphinic amide P═O vector (P1–O1) oriented *anti* with respect to the P═O of the phosphine oxide group, P2–O2. P2 and P3 are quasi coplanar with the oxygen atom of the second phosphinic amide moiety, O3, almost aligned with the P2–C25 vector (deviation from plane P2–O3–P3–C20 of 0.9(1)°) Interestingly, the O3···P2 distance of 2.990(2) Å is significantly shorter than the sum of the corresponding van der Waals radii

Table 1 Selected crystal data for (R_{P1}*,S_{P3}*)-**11** and complexes **12** and **13**

Compound	**11**	**12**	**13**
Empirical formula	C42 H51 N2 O3 P3	C44 H54 N6 O12 P3 Y	C86 H105 N8 O15 P6 Y
M	724.76	1040.75	1765.51
Crystal system	Monoclinic	Monoclinic	Triclinic
Space group	$P2_1/c$	$P2_1/c$	P-1
a/Å	13.567(2)	21.5641(7)	14.831(2)
b/Å	19.623(3)	20.9926(8)	15.879(2)
c/Å	14.296(2)	24.1037(8)	23.473(3)
α (°)	90	90	74.596(2)
β (°)	90.334(4)	119.372(2)	73.845(3)
γ (°)	90	90	62.892(3)
V/Å^3	3806.1(9)	9508.8(6)	4663.7
μ/mm^{-1}	0.198	1.395	0.792
D_c/g cm^{-3}	1.265	1.454	1.257
Crystal dimensions/mm	0.20 × 0.17 × 0.06	0.20 × 0.17 × 0.13	0.42 × 0.22 × 0.10
Z	4	8	2
T/K	150	100	150
F(000)	1544	4320	1852
θ range for data collection/°	1.50 to 25.71	1.08 to 24.46	0.92 to 24.45
Refls measured	19397	49562	24286
Refls unique	6271 (R_{int} = 0.0711)	15665(R_{int} = 0.0912)	15189(R_{int} = 0.0547)
Parameters/restraints	541/0	1189/0	1016/3
GOF on F^2	0.877	0.825	0.804
R_1 [$I \geq 2\sigma(I)$]	0.0446	0.0426	0.0576
wR_2 (all data)	0.0623	0.0754	0.1293
max./min. res. elec. dens./e Å^{-3}	0.349/−0.333	0.501/−0.823	1.178/−0.729

Table 2 Selected bond lengths (Å) and angles (°) for (R_{P1}*,S_{P3}*)-**11** and complexes **12** and **13**

(R_{P1}*,S_{P3}*)-**11**		**12**		**13**	
P1–O1	1.507(2)	Y1–O1	2.378(3)	Y1–O1	2.283(3)
P1–N1	1.588(2)	Y1–O1N1	2.484(3)	Y1–O2	2.335(3)
P1–C1	1.858(3)	Y1–O2	2.250(3)	Y1–O3	2.314(3)
P1–C7	1.844(3)	Y1–O2N1	2.412(3)	Y1–O4	2.330(3)
P2–O2	1.4232(16)	Y1–O3	2.233(3)	Y1–O5	2.319(3)
P2–C2	1.843(3)	Y1–O1N2	2.417(3)	Y1–O6	2.261(3)
P2–C19	1.927(3)	Y1–O2N2	2.461(3)	Y1–O7	2.431(3)
P2–C25	1.795(3)	Y1–O2N3	2.451(3)	Y1–O8	2.485(3)
P3–O3	1.537(2)	Y1–O1N3	2.459(3)	P1–O1	1.502(3)
P3–N2	1.594(2)	P1–N4	1.647(4)	P1–N1	1.637(4)
P3–C20	1.865(3)	P1–O1	1.513(3)	P2–O2	1.493(3)
P3–C31	1.792(3)	P2–O2	1.500(3)	P3–O3	1.498(3)
O1–P1–N1	108.34(12)	P3–N3	1.641(4)	P3–N2	1.631(4)
O1–P1–C1	112.21(12)	P3–O3	1.494(3)	P4–O4	1.507(3)
O1–P1–C7	108.39(12)	O1–Y1–O2	77.81(10)	P4–N3	1.639(4)
O2–P2–C2	113.57(12)	O1–Y1–O3	80.81(9)	P5–O5	1.489(3)
O2–P2–C19	113.42(11)	O2–Y1–O3	76.08(9)	P6–O6	1.498(3)
O2–P2–C25	110.00(11)	O1–P1–N4	117.98(18)	P6–N4	1.631(4)
O3–P3–N2	120.18(12)	O3–P3–N3	117.29(18)	O1–Y1–O2	73.05(10)
O3–P3–C20	115.40(12)	Y1–O1–P1	152.25(16)	O1–Y1–O3	97.79(11)
O3–P3–C31	109.77(13)	Y1–O2–P2	133.82(17)	O1–Y1–O4	88.97(11)
		Y1–O3–P3	158.24(17)	O1–Y1–O5	89.73(10)
				O1–Y1–O6	161.87(10)
				O1–Y1–O7	71.72(11)
				O1–Y1–O8	122.89(11)
				O1–P1–N1	112.6(2)
				O3–P3–N2	118.0(2)
				Y1–O1–P1	154.45(19)
				Y1–O2–P2	138.95(18)
				Y1–O3–P3	172.95(18)
				Y1–O4–P4	166.39(19)
				Y1–O5–P5	140.38(18)
				Y1–O6–P6	156.60(18)

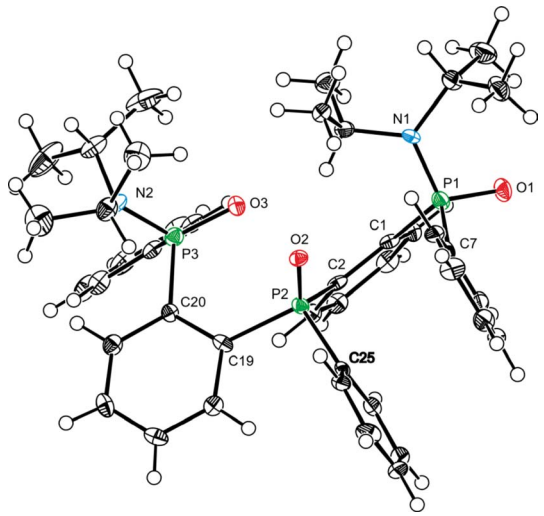

Fig. 5 ORTEP view of the crystal structure of (R_{P1}*,S_{P3}*)-**11** including the numbering scheme used. Thermal ellipsoids are shown at the 50% level.

(3.32 Å), which suggests the existence of a contact between these atoms. A similar interaction seems to be present in *ortho* phenyl-[22] and -naphthylbis(diphenylphosphine) dioxides[23] as well as in the solid state structure of the HI_3 adduct of the triphosphine trioxide ligand **5**.[24] The phosphorus atom geometries are tetrahedral, with min/max bond angles variations of 106.5(1)°–113.2(1)° for P1, 100.3(1)°–113.6(1)°for P2, and 101.5(1)°–120.2(1)° for P3. The O3···P2 contact noted above together with the almost linear arrangement of O3–P2–C25 (angle of 171.5(1)°) could be appropriate for considering P2 as a pentacoordinated atom with a trigonal bipyramid (tbp) geometry. However, several features indicate that the configuration of this atom is best described as tetrahedral: the O3–P2 distance is too long (2.990(2) Å), the sum of the bond angles comprising the equatorial atoms C2, C19, and O2 of the hypothetical tbp is only 339.0(3)°, the displacement of 0.41 Å of the P2 atom with respect to the quasi basal plane of the tbp, and perhaps most importantly, the lack of elongation of the P2–C25 bond anti to the O2 atom. The distance of 1.795(3) Å observed for this bond is of the same order[24] or even slightly shorter than those found in *P*-phenyl rings of related compounds.[22] As in other triarylphosphine oxides, the aromatic rings linked to P2 adopt a propeller-like arrangement. The nitrogen atoms show trigonal configuration as deduced from values of 350.7(6)° and 352.8(6)° for the sum of the bond angles of N1 and N2, respectively.

Bond distances in the phosphorus-containing functional groups are remarkable. The P–N bond lengths (average distance of 1.590(2) Å) are notably shorter than the values reported in *N*,*N*-dialkylphosphinic amides (average distance of 1.662 Å),[25] including some *ortho*-functionalised[19a,26] and *N*,*N*-diisopropyl derivatives.[20] As expected, the reduction in the P–N distance is accompanied by an appreciable increase of the P═O bond length (average distance of 1.522(2) Å) in the P(O)N linkage as compared with the mean value of 1.484 Å reported for analogue phosphinic amide moieties.[20,25,26] Significantly, the P3–O3 distance (1.537(2) Å) is slightly longer than that of P1–O1 as one would expect from the existence of a O3···P2.[27] Surprisingly, such interaction apparently produced a shortening of the P2–O2 bond in the phosphine oxide linkage (*cf.* the value of 1.423(2) Å *vs.* 1.489 Å in C_3P═O systems),[28] when a lengthening was expected. These facts suggests that the particular arrangement of the P═O groups in (R_{P1}*,S_{P3}*)-**11** is the result of electrostatic rather than covalent bonding interactions. Also relevant is the positioning of the oxygen atom of the phosphinic amide with respect to the nitrogen substituents, staggered for P3 and eclipsed with a methyl carbon for P1. As far as we know, (R_{P1}*,S_{P3}*)-**11** is the first example of a tridentate pincer ligand combining two P(O)N side arms connected to one PO group through a scaffold of *ortho*-substituted phenyl rings that has been ever characterised in the solid state.

The infrared spectrum of complex **12** (KBr disk) displays bands at 1190 (s) and 986 (m) cm^{-1} assigned to the P═O and P–N stretching vibrations, respectively.[11–13,16,29] The shift of these absorptions to lower frequencies for the P═O (~ 20–36 cm^{-1})[30] and to higher frequencies for the P–N (~8 cm^{-1}) with respect to the corresponding bands in the free ligand, support the binding to the yttrium cation. Absorptions typical of coordinated nitrate were observed at 1482 (s), 1295 (s), 1058 (w) and 817 (w) cm^{-1}. However, the unequivocal identification of the coordination mode of NO_3^- groups to the metal is not possible.

Single crystals of the 1 : 1 complex [Y(R_{P1}*,S_{P3}*)-**11**)$(NO_3)_3$], **12**, were prepared from an acetonitrile solution layered with diethyl ether. After 12 h at room temperature crystalline material suitable for X-ray diffraction was obtained. A view of the molecule is shown in Fig. 6. Selected crystal data and bond lengths and angles are given in Tables 1 and 2, respectively, as the two independent molecules in the asymmetric unit do not differ significantly, we use one of them on the structural discussion. The Y(III) is coordinated to three bidentate NO_3 and one tridentate ligand (R_{P1}*,S_{P3}*)-**11** resulting in a nine-coordinate polyhedron that approximates to a tricapped trigonal prism (Fig. 7a).[31] Similar coordination polyhedra have been reported for 1 : 1 complexes of a *meso* diphosphine dioxide ligand of type **3** (Fig. 2) with $Nd(NO_3)_3$ and $Er(NO_3)_3$.[32] Replacing conceptually the nitrate groups by an hypothetical monoatomic ligand transforms the nine-coordinated polyhedron into a pseudo-octahedron that can be viewed as a *fac* isomer, *i.e.* the three P═O moieties define a face of an octahedron with all three groups *ca.* 90° apart from each other (Fig. 6b).

The nitrates are symmetrically coordinated to Y(III) and the Y–O(nitrates) distances (av. 2.448 Å) are comparable to those in $[Y(R_3PO)_3(NO_3)_3]$ (R_3PO = Ph_3PO, Ph_2MePO, Me_3PO)[16c] and related structures of complexes of lanthanide nitrate and phosphine oxides.[6a,e,33] As expected, the geometry shows that the nitrate coordinated oxygen atoms have longer N–O distances (average 1.258 Å) than the uncoordinated or "free" N–O and that the O–N–O angles are close to the idealized 120° of isolated NO_3 anions (min/max variation of 115.4(4)°–122.8(4)°). In complex **12** the tripodal ligand is coordinated by the three phosphinoyl moieties with Y–O–P angles of 152.2(2)°, 133.8(2)°, and 158.2(2)° for P1, P2 and P3 respectively. The complex has C_1 symmetry as is evidenced by the different conformation of the two seven-membered metallacycles formed by binding the P═O groups of ligand **11** to the Y(III) ion. Although both metallacycles acquire a slightly twisted envelope conformation in the crystal, the "flap" of the envelope is defined only by the yttrium atom for the ring involving P2, O2, P3, and O3, whereas this flap includes the O1–Y1–O2 moiety for the ring containing the P1═O1 and P2═O2 groups.[34] The asymmetry of the complex is also reflected in the large difference in the intraligand O···O distances (2.908(4) Å for O1···O2 *vs.* 2.763(4) Å for O2···O3). The phosphorus

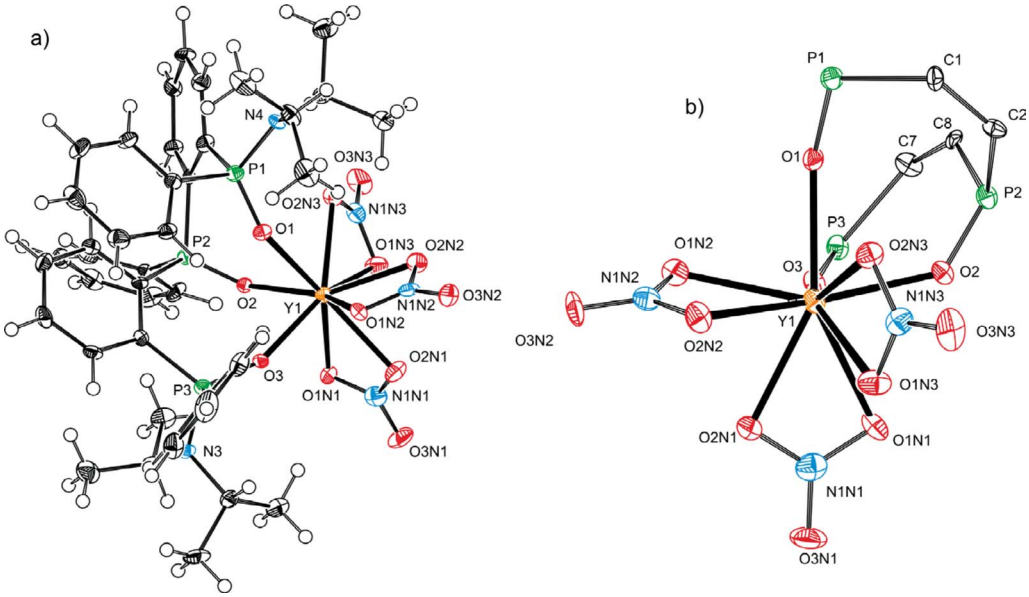

Fig. 6 a) ORTEP view of the crystal structure of complex [Y((R_{P1}*,S_{P3}*)-**11**)$(NO_3)_3$], **12** including the numbering scheme used (ellipsoids drawn at 50% probability). b) Coordination sphere drawing of **12**.

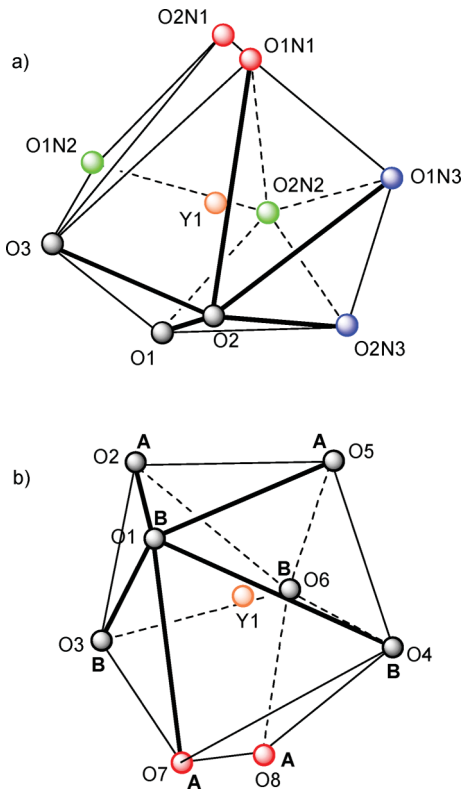

Fig. 7 Shape of the coordination polyhedron of a) **12** and b) **13**.

atoms retain the characteristics observed in the free ligand, *i.e.*, tetrahedral configuration (range of bond angles of 103.8(2)° to 117.4(2)°) and propeller-like arrangement of the aryl rings linked to P2. Tridentate chelation of **11** with Y(III) involves a rotation around the P1–C1 bond of the ligand. This reorganization of the chelate chain places the phenyl ring bonded to P1 almost parallel to the *ortho* substituted ring connected to P2 and P3 (distance of centroids of 3.592 Å, angles between centroids and the *para* carbons C11 and C16 of 88.1° and 98.8°, respectively). The asymmetry of the molecule also extends to the P═O and Y–O(P) distances, which are all different. The Y–O(P) distances, 2.378(3), 2.250(3) and 2.233(3) Å for O1, O2 and O3, respectively, are comparable with the related bond lengths found in complexes of yttrium nitrate and phosphine oxides.[16c] It is worthy of note that the binding to both phosphinic amide groups is clearly different (Δ = 0.145 Å). Interestingly, the expected lengthening of the P–O bonds produced by the coordination of the P═O groups[5b,e,35] to the Y^{3+} cation is only observed for P1–O1 (1.513(3) Å) and P2–O2 (1.500(3) Å). Furthermore, the increase is notably larger for the phosphine oxide linkage (Δ = 0.0768 Å) than for the phosphinic amide P1–O1 bond (Δ = 0.006 Å). In sharp contrast, the P3–O3 bond distance (1.494(3) Å) in complex **12** decreases markedly (Δ = –0.043 Å) with respect to the length found in the free ligand **11**. This behaviour has no precedent in the coordination of tridentate ligands such as **3**,[8] **4**,[9] and **5**[10] with lanthanide cations. Curiously, the P–N distances in **12** are larger than in **11** and comparable to those described for uncomplexed *N*,*N*-dialkylphosphinic amides.[25,26] The variations in P═O bond lengths mentioned suggest that the phosphine oxide P═O of tridentate ligand **11** binds to the Y^{3+} cation more strongly than the P═O linkage of the P(O)N groups. A definite explanation for these observations is not available at the moment.

The infrared spectrum of the 2 : 1 complex [Y((R_{P1}*,S_{P3}*)-**11**)$_2(NO_3)$][$(NO_3)_2$, **13**, in KBr showed similar features to that of the 1 : 1 complex **12** for the P═O (1173 cm^{-1}) and P–N (986 cm^{-1}) stretching absorptions. Bands for coordinated NO_3^- are observed at 1469 (m), 1310 (m), 1057 (w) and 817 (w) cm^{-1}. Characteristic bands for the unbound nitrate group appear at 1384 (s) and 829 (w) cm^{-1}. As for **12**, crystals of **13** suitable for X-ray analysis were obtained by layering diethyl ether on a concentrated acetonitrile solution of **13**. A view of the molecule is shown in Fig. 8. Selected crystal data and bond lengths

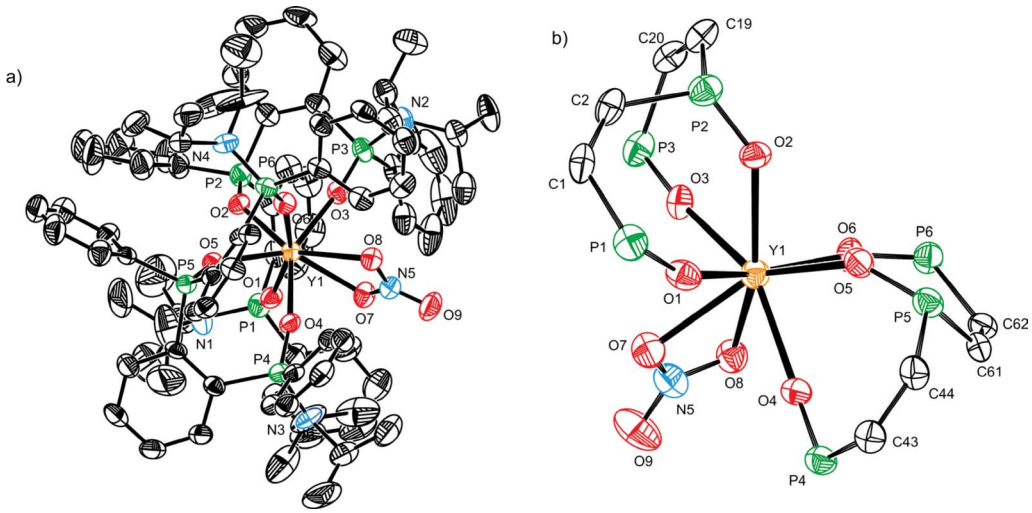

Fig. 8 a) ORTEP view of the crystal structure of cation $[Y((R_{P1}*,S_{P3}*)\text{-}\mathbf{11})_2(NO_3)]^{2+}$ of **13** including the numbering scheme used (50% thermal ellipsoids). Hydrogens, the two outer nitrate ions and one molecule of acetonitrile used in the recrystallization were omitted for clarity. b) Coordination sphere drawing of **13**.

and angles are presented in Tables 1 and 2. The solid-state structure confirms that two ligands $(R_{P1}*,S_{P3}*)$-**11** bound to the Y^{3+} cation by displacing two nitrate ions and all water molecules from the inner coordination sphere of $Y(NO_3)_3{\cdot}6H_2O$. The outer coordination sphere consists of two nitrate ions and one molecule of acetonitrile used in the recrystallization. The eight-coordinate polyhedron formed by the two tridentate chelates and the bidentate nitrate represents a dodecahedron of triangular faces.[31] The oxygen atoms of the phosphine oxide linkages occupy A edges whereas those of the P(O)N groups are placed in adjacent B positions of an ideal dodecahedron (Fig. 8b).[36] The two *meso* ligands show a face-to-face *syn* arrangement of the phosphorus atoms of opposite relative configuration. The remaining two A positions of the dodecahedron are occupied by the oxygen atoms of the bidentate nitrate ion. A simplified view of the coordination mode of the tridentate ligands can be obtained by artificial elimination of nitrate coordination to yttrium. The resulting coordination polyhedron (Fig. 8b) would approximate to a distorted octahedron with a *fac* coordination of the ligands in which phosphine oxides and chiral phosphinic amide moieties of opposite configuration from each ligand are arranged *syn* to each other.

The complex has C_1 symmetry. The conformation adopted by the tridentate ligands bound to Y^{3+} in complex **13** is analogous to that found in the 1 : 1 complex **12**, *i.e.*, twisted envelope seven-membered matallacycles. Taking as reference the O3–Y1–O6 atoms defining a plane, the oxygen atoms O2 and O1 bisect the angles O6–Y1–O5 and O5–Y1–O4, respectively, and are allocated perpendicularly above those planes.

The P–X (X = O, N) distances show the same features noted in complex **12**. Perhaps the most relevant characteristic is the very small differences of lengths among bonds of the same type: 1.498(4)–1.507(4) Å and 1.631(4)–1.639(4) Å for P–O and P–N bonds of P(O)N groups, respectively, and 1.493(3) Å and 1.489(3) Å for the respective phosphine oxide P2–O2 and P5–O5 bonds. The latter are similar to those reported for 2 : 1 complexes of Eu^{3+},[8b,37] Nd^{3+},[8c,32] Th^{3+}, and Yb^{3+} nitrates[8a] with tridentate ligands **3** as well as complexes of cerium(III) nitrate with ligand **4**.[9b,c] The Y–O distances are all different and fall in the same ranges found in **12** for O(P) (2.261(3)–2.335(3) Å) and O(N) (2.431(3) and 2.485(3) Å) oxygen atoms. Curiously, the shortest Y–O distances arise from the oxygen atoms of phosphinic amide groups of relative *R* configuration (values of 1.283(3) Å for Y1–O1 and 2.261(3) Å for Y1–O6). The intraligand O···O distances are quite regular, with the same ligand showing the two extreme values (2.712(4) Å (O2···O3) to 2.748(5) Å (O1···O2)). The geometry of the phosphorus and nitrogen atoms can be described as tetrahedral and trigonal, respectively. Notwithstanding, some bond angles depart notably from ideal values of these configurations. The maxima deviations are observed for P5 (range of values of 103.5(2)°–119.5(2)°) and N3 (range of values of 113.35°–129.88°).

Solution state characterisations

The structure of compound **11** in CD_3CN solution was established based on standard NMR spectroscopic methods. The presence of two phosphinic amide fragments connected through a phosphine oxide bridge was readily deduced from the two signals observed in the ^{31}P NMR spectrum, one triplet at δ_P 37.16 and one doublet at δ_P 31.61 ppm in a ratio of 1 : 2 and a mutual coupling constant $^3J_{PP}$ of 8.1 Hz. The prochirality of the molecule turns the methyl protons of the *N*-isopropyl groups into diastereotopic ones. They appear in the ^1H NMR spectrum as two doublets at δ_H 1.12 and 1.15 ppm due to the coupling with the adjacent CH proton ($^3J_{HH}$ 6.9 Hz). The four equivalent methynes show a characteristic double heptet at δ_H 3.51 ppm originating from the coupling of the methyl protons and the phosphorus nucleus ($^3J_{HH}$ 6.9 Hz, $^3J_{PH}$ 6.8 Hz). The corresponding carbons are observed in the ^{13}C NMR spectrum at δ_C 23.22 and 23.81 ppm for the methyl carbons and δ_C 47.7 ppm for the methyne groups. The aromatic region of this spectrum is characterised by 14 resonances in the range of δ_C 126–139 ppm.

The ^{31}P NMR analysis of $[Y((R_{P1}*,S_{P3}*)\text{-}\mathbf{11})(NO_3)_3]$ (**12**) indicated that the asymmetry of the ligand established in the solid state was retained in solution. The ^{31}P spectrum of a *ca.* 0.1 M

acetonitrile solution of **12** at room temperature consisted of three signals with the same integral: a double triplet at δ_P 42.67 ($^3J_{PP}$ 7.7, $^2J_{YP}$ 5.4 Hz) ppm, and two broad triplets at δ_P 35.98 and 33.44 ppm. The multiplicity pattern observed clearly indicates that the ligand is acting as a tridentate chelate. The signal at δ_P 42.67 ppm can be unequivocally assigned to the ^{31}P of the phosphine oxide linkage coupled to two P(O)N groups and one Y^{3+} cation. As for the phosphinic amide phosphorus, the coupling constants with the vicinal P═O group and the yttrium ion seem to be of approximately the same magnitude. The inequivalence of the phosphinic amide substructures in **12** is also ascertained in the ^{1}H NMR spectrum. The *N*-isopropyl groups afford two sets of signals. One appears as a relatively broad pair of doublets (δ_H 0.77, 0.94 ppm, $^3J_{HH}$ = 6.0 Hz) and one heptet (δ_H 3.36 ppm, $^3J_{HH}$ = 6.0 Hz) as expected for two diastereotopic methyl groups and one methyne proton, respectively. The second group of isopropyl signals shows the methyl (δ_H 1.05 and 1.18 ppm) and methyne (δ_H 3.67 ppm) resonances as very broad signals without resolvable homo- or hetero-nuclear coupling constants.[38] The features noted in the ^{1}H and ^{31}P NMR spectra indicate the existence of some dynamic process in complex **12**. This dynamic behaviour is even more pronounced in the ^{13}C NMR spectrum, where the signals of one N^iPr_2 fragment seem to have reached coalescence at room temperature and could not be detected.

A variable temperature ^{31}P NMR study was undertaken to get some insight into the dynamic behaviour of **12** (Fig. 9). For simplicity, the ^{31}P signals were labelled with the same numbers employed in the solid-state structure. Increasing the temperature to 75 °C produced the collapse of P1 and P3 into a single average broad signal at δ_P 34.7 ppm. This means that at this temperature any hindered rotations around the P–N linkages and conformational exchange processes between metallacycles involving the P(O)N linkages are occurring rapidly on the NMR time scale. Binding of the ligand to Y^{3+} at this temperature is evidenced by the ^{89}Y,^{31}P coupling shown by P1 ($^3J_{PP}$ = $^2J_{YP}$ = 7.7 Hz). P1 and P3 exhibit different behaviour at low temperature. In both cases, the coupling information is apparently lost. P1 undergoes deshielding and achieves the minimum line width at 0 °C ($W_{1/2}$ = 26 Hz), while P3 is shifted to lower frequencies and the sharpest signals is obtained at –40 °C ($W_{1/2}$ = 23 Hz). Aggregation effects could be discarded by repeating the study using a very dilute sample. Using a *ca.* 10 mM solution of **12** in acetonitrile afforded the same results, thus confirming the absence of concentration dependent processes. At the end of the study, the room temperature spectrum is recovered showing that the dynamic processes observed are fully reversible.

Perhaps the most relevant NMR issue in yttrium complexes is ^{89}Y NMR. The large chemical shift range reported for this metal nucleus, *ca.* 1300 ppm, suggests that should be a good reporter of small changes in its coordination sphere.[39] The ^{89}Y nucleus combines attractive properties for high resolution NMR, *i.e.*, spin I = 1/2, 100% natural abundance, with severe limitations for rapid accessing to NMR data: low receptivity (D^C = 0.7) and long T_1 relaxation times.[39,40] The need to use long recovery delays in standard excitation–acquisition ^{89}Y NMR experiments has been overcome by transferring polarization from ^{1}H to ^{89}Y *via* INEPT[41] and DEPT[42] schemes or using inverse detection through proton.[43] Recently, we have reported the application of inverse ^{31}P detection experiments for obtaining ^{89}Y NMR data of yttrium(III) complexes with triphenylphosphine oxide.[44]

The ^{31}P,^{89}Y{^{1}H} HMQC spectrum of **12** measured at 20 °C, 0 °C and –40 °C is displayed in Fig. 10. At 20 °C only P2 shows a correlation with a Y^{3+} cation at δ_Y of –2.5 ppm. Most probably, the rather large line width of P1 and P3 prevents the detection of any ^{31}P,^{89}Y correlation due to rapid transverse relaxation. This hypothesis is confirmed by acquiring the spectrum at 0 °C and –40 °C, the temperatures corresponding to the narrowest P1 and P3 signals, respectively (see above). Under these conditions the correlations of P1/P2 and P1/P3 with the ^{89}Y nucleus are clearly observed, which also reveal a very small temperature dependence

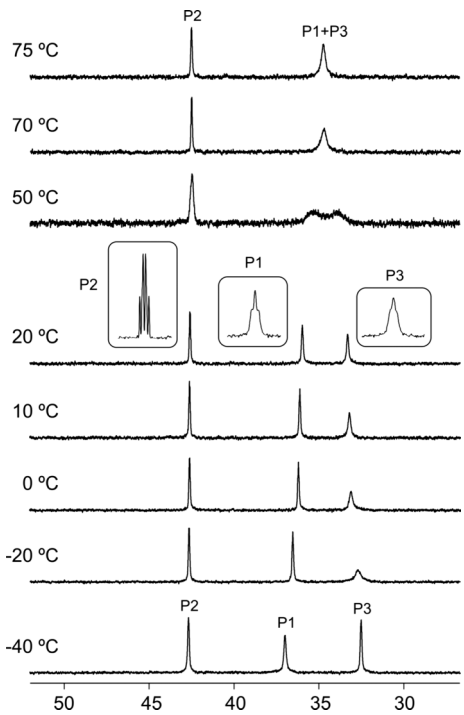

Fig. 9 ^{31}P NMR (202.5 MHz) spectra as a function of temperature for a *ca.* 0.1 M sample of **12**, in CD_3CN.

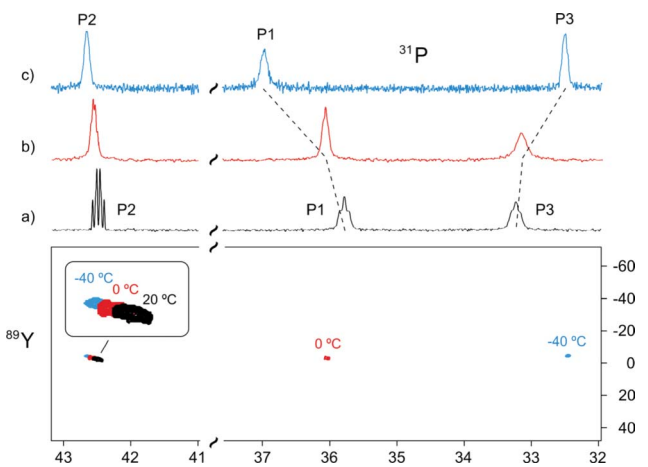

Fig. 10 ^{31}P,^{89}Y{^{1}H} HMQC (202.5 MHz) spectra of a sample of **12** *ca.* 0.1 M in CD_3CN measured at 20 °C (a), 0 °C (b), and –40 °C (c). Top projections correspond to ^{31}P NMR spectra acquired at the temperature indicated in the inset of the 2D spectrum. Experimental time *ca.* 3 h.

of δ_Y ($\Delta\delta_Y$ = −1.8 ppm for a ΔT= −60 °C). These results are consistent with an Y^{3+} cation coordinated in a κ^3-O fashion to ((R_{P1}*,S_{P3}*)-**11**, in agreement with the solid-state structure.

The ^{31}P NMR spectrum of the 2 : 1 complex **13** consist of three signals: a double triplet for P2 (δ_P 42.01 ppm, $^3J_{PP}$ 8.4, $^2J_{YP}$ 5.6 Hz) and two triplets for P1 (δ_P 40.30 ppm, $^3J_{PP} = {}^2J_{YP}$ 8.4 Hz) and P3 (δ_P 34.28 ppm, $^3J_{PP} = {}^2J_{YP}$ 8.4 Hz) (see Fig. 4). This pattern is comparable to the spectrum obtained for the 1 : 1 derivative. In this case, only P3 appears significantly broadened probably due to rapid transverse relaxation induced by the ^{14}N of the nitrate ligand. As for **12**, P2 is readily assigned based on the double triplet produced by the coupling with two ^{31}P of the P(O)N linkages and the ^{89}Y nucleus. The presence of only three signals in the spectrum indicates that the two ligands in **13** are equivalent. This means that the solid-state structure is retained in solution and the flexibility of the ligands produces an average structure that can be considered as a *meso* species with a plane of symmetry including the nitrate ligand. The binding of all P═O groups to Y^{3+} is demonstrated by the ^{89}Y,^{31}P coupling displayed by all resonances. The existence of these couplings are the basic requirement for performing the ^{31}P,^{89}Y{^{1}H} HMQC experiment. The spectrum acquired using a compromise delay of 41.7 ms (appropriate for $^2J_{YP}$ 12 Hz) for the preparation of anti-phase magnetization is given in Fig. 10a.[45] In this way, the three phosphorus signals show a correlation with an yttrium at a δ_Y −23.5 ppm. This value represents a shielding of the yttrium nucleus of 21 ppm as compared with **12**, in agreement with the empirical group contributions to δ_Y estimated for phosphine oxide ligands.[39b] The ^{1}H NMR spectrum of **13** also exhibited averaged signals for the two ligand molecules incorporated in the complex. The analysis, in combination with the ^{1}H,^{31}P gHMQC spectrum, allowed the assignment of the proton signals of the different phosphinic amide fragments.

The different ^{89}Y chemical shift of the 1 : 1 and 2 : 1 complexes is an indirect evidence of yttrium coordination to two tridentate ligands in the latter. An unequivocal proof of the number of P═O groups bound to yttrium(III) in **13** would be provided by the multiplicity of the ^{89}Y signal. This information was readily obtained from the ^{89}Y,^{31}P{^{1}H} DEPT experiments. The heptet observed in the spectrum acquired without using ^{31}P decoupling during acquisition clearly demonstrated the coupling of Y^{3+} to six ^{31}P, as expected in complex **13** (Fig. 11b). The multiplet collapsed to a singlet when the spectrum was measured including ^{31}P decoupling, thus confirming that the splitting observed arises from ^{89}Y,^{31}P coupling (Fig. 11c). As far as we know, these experiments represent the first application of direct observation of ^{89}Y NMR with intensity enhancement through polarization transfer from ^{31}P. Besides the increment of intensity afforded by the polarization transfer technique, the repetition delay is determined by the relaxation time of the ^{31}P, much shorter than that of ^{89}Y. Both factors contribute to reduce the experimental time required for accessing to ^{89}Y NMR data as compared with the standard excitation scheme.

Additional insights into the solution structure of the yttrium complexes **12** and **13** were obtained *via* diffusion studies. The measurement of diffusion constants *via* pulsed gradient spin-echo (PGSE) NMR methods[46] has recently attracted increasing interest as this technique provides data on molecular volumes, and thus indirectly, on structural characteristics.[47] The major advantage of this method compared with, for instance, colligative measurements is that experimental parameters such as temperature or concentration can be adapted to the requirements. In addition, the sequences needed are available in a standard NMR spectrometer facilitating the performance of the experiment. Table 3 shows pulsed field gradient spin-echo (PGSE) diffusion data for **12** and **13** in acetonitrile solution. For the diffusion studies presented, two model system with different steric hindrance were employed, *i.e.*, the partially deuterated acetonitrile as an internal standard, and the neutral ligand **11** as an external one. In the traditional Stejskal–Tanner plots (Fig. 12), the less the attenuation, the lower the diffusion coefficient, the larger the molecular size.

From the measured D value at *ca.* 0.1 M samples for **12** and **13**, and saturated solution in the case of **11**[48] we estimate (*via* the Stokes–Einstein equation) the hydrodynamic radius r_H to be 7.4, 8.8 and 5.8 Å, for complexes **12**, **13**, and ligand **11**, respectively, which are in reasonable agreement with the values derived from the crystallographic data given that solvent molecules and non-bonded nitrates included in the solid-state lattice cannot be excluded from the $r_{X\text{-ray}}$ calculation.

For two spherical molecules, in which one has twice the volume of the other, one expects the ratio of the slopes (or D-values) to be $(2)^{1/3} \approx 1.26$. Assuming that the smaller is of spherical shape and the larger species has an elongated shape (the longer axis being twice

Table 3 Diffusion coefficient (D) and hydrodynamic radius (r_H) values for ligand (R_{P1}*,S_{P3}*)-**11** and complexes **12** and **13** at room T/K in CD_3CN

Compounds	$D^a \times 10^{10}$ m^2 s^{-1}	r_H (Å)^b	$r_{X\text{-ray}}$ (Å)^c
12	7.912	7.4	6.6
13	6.636	8.8	8.2
(R_{P1}*,S_{P3}*)-**11**	10.138	5.8	5.9
CH_3CN	34.330^d	1.7	

^{a} The experimental error in the D values is ±2%. ^{b} The viscosity η used in the Stokes–Einstein equation was taken from Perry's Chemical Engineers' Handbook 8th Edition (www.knovel.com) and is 0.3635 × 10^{-3} kg m^{-1} s^{-1}. ^{c} Deduced from the X-ray structure by considering the volume of the crystallographic cell divided by the number of contained asymmetric units, the latter one is assumed to be spherical in shape. ^{d} Average value considering the same signal in the three different samples based on (R_{P1}*,S_{P3}*)-**11**, **12** and **13**.

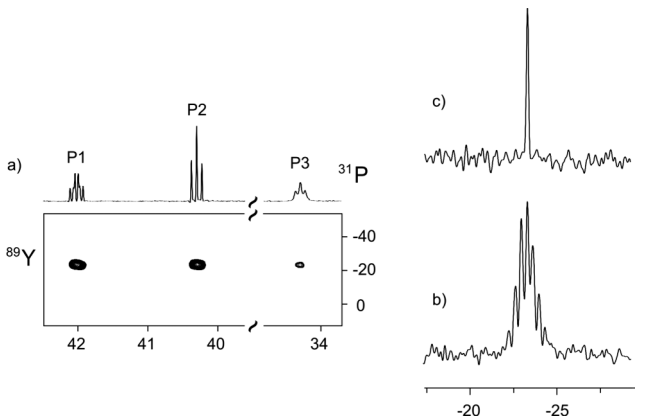

Fig. 11 (a) ^{31}P,^{89}Y{^{1}H} HMQC (202.5 MHz) spectrum of **13** *ca.* 0.1 M in CD_3CN measured at 20 °C, experimental time 3 h. (b) ^{89}Y,^{31}P{^{1}H} DEPT (24.507 MHz) spectrum of **13** *ca.* 0.1 M in CD_3CN measured at ambient temperature without ^{31}P decoupling during acquisition, (10240 scans, experimental time of 14 h). (c) The same experiment as (b) acquired with ^{31}P decoupling (1299 scans, experimental time 2 h).

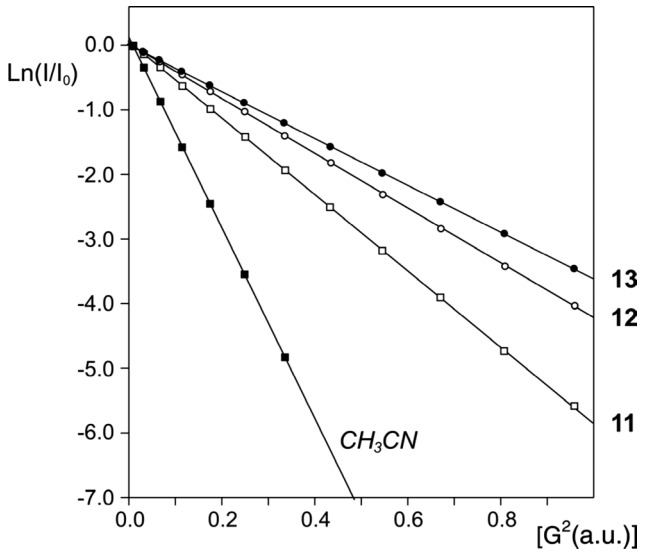

Fig. 12 Stejskal–Tanner plots from ^{1}H PGSE diffusion experiments in CD_3CN at room temperature using the stimulated echo sequence of complexes **12** (○) and **13** (●), precursor **11** (□), and partially deuterated acetonitrile (■), the latter as internal standard. The solid lines represent linear least-squares fits to the experimental data.

that of the smaller), the ratio is then of *ca*. 1.18.[49] The experimental ratio of *D*-values of 1.19 (Table 3) is consistent with **13** having *ca*. twice the volume of **12**. The small fluctuation can be rationalised by taking into account the possible contributions of the nitrate ions. They can be completely separated by solvent or at least partially paired regarding the cationic entity. Together with this the exchange between free and bound nitrates can not be excluded, which could represent a source of uncertainty. The diffusion data obtained for **11** fit reasonably well with the radius calculated from the solid-state structure, and provide a clear picture of how the size of the molecule increases when the ligand itself binds to one $Y(NO_3)_3$ fragment.

Conclusions

The diastereoselective synthesis of the *meso* tridentate ligand (R_{P1}*,S_{P3}*)-**11** containing two *ortho*-substituted diphenylphosphinic amides connected through a PhP═O moiety and its successful coordination to yttrium(III) nitrate to give 1 : 1, [Y((R_{P1}*,S_{P3}*)-**11**)$(NO_3)_3$] **12**, and 2 : 1, [Y((R_{P1}*,S_{P3}*)-**11**)$_2(NO_3)](NO_3)_2$ **13**, complexes is described for the first time. The new compounds have been characterised in the solid-state through X-ray diffraction analysis. A detailed multinuclear magnetic resonance study afforded key aspects of the synthesis and solution structure of **12** and **13**. Complex **12** is the product of thermodynamic control of the 1 : 1 reaction between ligand **11** and yttrium nitrate, whereas the derivative **13** is formed diastereospecifically in about 5 min when a 2 : 1 molar ratio of ligantd to Y(III) salt is used. Both complexes retain in solution the same structure found in the solid-state. Binding of one or two ligands to Y^{3+} has been ascertained through ^{31}P,^{89}Y-HMQC and ^{89}Y,^{31}P-DEPT NMR experiments, which provided rapid access to ^{89}Y NMR data making use of ^{31}P for inverse detection or as source of polarization transfer, respectively. In addition, NMR diffusion measurements contributed to the understanding the nuclearity in solution of both **12** and **13**. Extension of the present chemistry to f-block elements is currently under study in our laboratories.

Methods and materials

Unless stated otherwise, all operations were performed using standard Schlenk techniques under an inert atmosphere of nitrogen. The solvents were dried prior to use in a Pure Solv 400-4-MD system, according to the procedure described by Pangborn and Grubbs.[50] Commercial reagents, except *n*-butyllithium, were distilled prior to use. TMEDA was distilled from KOH.

^{1}H (300.13 MHz), ^{13}C (75.47 MHz), and ^{31}P (121.47 MHz) NMR spectra were recorded in $CDCl_3$ and CD_3CN except otherwise stated, on a Bruker Avance DPX300 equipped with a QNP ^{1}H/^{13}C/^{19}F/^{31}P probe. 2D ^{31}P,^{89}Y{^{1}H} HMQC and 1D ^{89}Y,^{31}P{^{1}H} DEPT spectra were acquired on a Bruker Avance 500 spectrometer (^{89}Y, 24.5 MHz; ^{31}P, 202.4 MHz) using a direct TBO (^{1}H/^{31}P/BB) probe head. Chemical shifts are reported in ppm with respect to tetramethylsilane for ^{1}H and ^{13}C using the solvent signal as reference, to external 85% H_3PO_4 for ^{31}P and to external $Y(NO_3)_3{\cdot}6H_2O$ for ^{89}Y. Standard Bruker software was used for acquisition and processing routines. Infrared spectra were recorded in a Mattson–Genesis II FTIR equipment. High resolution mass spectra were recorded on Agilent Technologies LC–MSD TOF and HP 1100 MSD equipment with electrospray ionization. Compounds **6**,[19a,51] has been described previously. Melting points were recorder on a Büchi B-540 capillary melting point apparatus and were uncorrected.

Diffusion measurements were performed using the Stimulated Echo Pulse Sequence[52] on a Bruker Avance 500 without spinning. The shape of the gradient pulse was rectangular, and its strength varied automatically in the course of the experiments. The calibration of the gradients was carried out *via* a diffusion measurement of HDO in D_2O, which afforded a slope of 2.022×10^{-4}. To check reproducibility, three different measurements with different diffusion parameters (δ and/or Δ) were always carried out. The gradient strength was increased in 8% steps from 10% to 98%.

Preparation of (R_{P1}*,S_{P3}*)-11

To a solution of TMEDA (0.55 mL, 3.7 mmol) and phosphinic amide **6** (1 g, 3.32 mmol) in dry toluene (50 mL), at –90 °C, was added *n*-BuLi (2.28 mL, 3.6 mmol, 1.6 M in hexane) dropwise. After one hour of deprotonation, $PhP(O)Cl_2$ (0.26 mL, 1.66 mmol) was added and the reaction was stirred overnight out of the cold bath. Then, the solvent was evaporated under vacuum and the residue was poured into water (100 mL) and extracted with dichloromethane (3 × 25 mL). The organic layers collected were washed five times with 50 mL of distilled water, dried with Na_2SO_4, filtered, and concentrated in vacuum to give a yellow–brown residue from which a brown precipitate was obtained upon addition of Et_2O (150 mL). The product was filtered and washed up three times with Et_2O providing 660 mg (55% isolated yield) of a white solid that was used further in complexation reactions. Mp 168–169 °C. IR (KBr disk): ν_{max}/cm^{-1} 979 (s), 1102 (s), 1111 (s), 1209 (s), 1227 (s). ^{1}H NMR ($CDCl_3$ δ): 1.12 (d, 12H, $^{3}J_{HH}$ 6.9 Hz, 4CH_3), 1.16 (d, 12H, $^{3}J_{HH}$ 6.9 Hz, 4CH_3), 3.54 (dh, 4H, $^{3}J_{HH}$ 6.8 Hz, $^{3}J_{PH}$ 6.8 Hz, 4CH), 6.98 (ddd, 2H, $^{3}J_{HH}$ 7.3 Hz, $^{3}J_{HH}$

7.2 Hz, $^4J_{PH}$ 3 Hz, ArH), 7.12 (m, 1H, ArH), 7.23 (m, 4H, ArH), 7.3 (m, 2H, ArH), 7.32 (m, 2H, ArH), 7.44 (m, 2H, ArH), 7.53 (m, 2H, ArH), 7.55 (m, 4H, ArH), 7.99 (dddd, 2H, $^3J_{HH}$ 7.6 Hz, $^4J_{HH}$ 0.9 Hz, $^4J_{PH}$ 4 Hz, $^3J_{PH}$ 12 Hz, ArH), 8.11 (m, 2H, ArH). ^{13}C NMR ($CDCl_3$ δ): 23.22 (d, $^3J_{PC}$ 3 Hz, $4CH_3$), 23.81 (d, $^3J_{PC}$ 3 Hz, $4CH_3$), 47.7 (d, $^2J_{PC}$ 4.8 Hz, 4CH), 126.41 (d, $^3J_{PC}$ 13.2 Hz, 2C*Ar*), 127.41 (d, $^3J_{PC}$ 12.6 Hz, 4C*Ar*), 129.63 (dd, $^4J_{PC}$ 3 Hz, $^3J_{PC}$ 11.4 Hz, 2C*Ar*), 129.68 (dd, $^4J_{PC}$ 3 Hz, $^3J_{PC}$ 12.4 Hz, 2C*Ar*),130.14 (d,,$^43J_{PC}$ 3 Hz, C*Ar*), 130.54 (d, $^4J_{PC}$ 2.4 Hz, 2C*Ar*), 132.63 (d, $^2J_{PC}$ 10.2 Hz, 2C*Ar*), 132.89 (d, $^2J_{PC}$ 9.8 Hz, 4C*Ar*), 134.06 (dd, $^2J_{PC}$ 10.1 Hz, $^3J_{PC}$ 10.1 Hz, 2C*Ar*), 134.67 (d, $^1J_{PC}$ 118.3 Hz, $2C_{ipso}$), 136.24 (d, $^1J_{PC}$ 104.6 Hz, C_{ipso}), 137.7 (dd, $^1J_{PC}$ 124.4 Hz, $^2J_{PC}$ 9 Hz,$2C_{ipso}$), 137.77 (dd, $^2J_{PC}$ 11.4 Hz, $^3J_{PC}$ 11.4 Hz,C-8/C-5), 138.89 (dd, $^1J_{PC}$ 102.6 Hz, $^2J_{PC}$ 10.6 Hz,$2C_{ipso}$). ^{31}P NMR ($CDCl_3$ δ): 31.61 (d, $^3J_{PP}$ 6.1 Hz), 37.16 (t, $^3J_{PP}$ 6.1 Hz). MS *m*/*z*: 725(M + 1). Analysis: calcd (%) for $C_{42}H_{51}N_2O_3P_3$: C, 69.60; H, 7.09; N 3.87. Found: C, 69.64; H, 7.30; N, 3.88. Crystals suitable for X-ray analysis were obtained from a chloroform solution (20 mg in 0.5 mL) layered with diethyl ether (1 mL).

General procedure for the preparation of complexes [Y((R_{P1}*,S_{P3}*)-11)$(NO_3)_3$] (12) and [Y((R_{P1}*,S_{P3}*)-11)$_2(NO_3)$][$(NO_3)_2$ (13)

To a suspension of (R_{P1}*,S_{P3}*)-**11** (58 mg, 0.08 mmol) in 0.75 mL MeCN was added $Y(NO_3)_3{\cdot}6H_2O$ (15.3 mg (0.04 mmol) for **12**; or 30.6 mg, 0,08 mmol for **13**). After 15 min of stirring (for **13**) or 4 days (for **12**) the reaction was complete. Slow evaporation of the corresponding solutions afforded the complexes **12** and **13** as air stable solids in more than 97% of purity. Crystals suitable for X-ray analysis were obtained from acetonitrile solutions layered with diethyl ether.

[Y((R_{P1}*,S_{P3}*)-11)$(NO_3)_3$] (12). Mp 220–221 °C (dec.). IR (KBr disk): ν_{max}/cm^{-1} 817 (w), 985 (m), 1057 (w), 1190 (s), 1295 (s), 1384 (m), 1482 (s). ^{1}H NMR (CD_3CN, δ): 0.75 (br, 6H, $2CH_3$), 0.92 (br, 6H, $2CH_3$), 1.01 (br, 6H, $2CH_3$), 1.17 (br, 6H, $2CH_3$), 3.35 (br, 2H, 2CH), 3.65 (br, 2H, 2CH), 6,31 (br, 2H, ArH), 6.46 (br, 1H, ArH), 6.62 (br, 1H, ArH), 7,22 (br, 6H, ArH), 7.51 (br, 2H, ArH), 7.75 (br, 6H. ArH), 8.02 (br, 1H, ArH), 8.31 (br, 3H, ArH), 8.53 (br, 1H, ArH). ^{13}C NMR (CD_3CN, δ): 22.25 (br, $2CH_3$), 22.93 (br, $2CH_3$), 48.93 (br, 2CH), 137.79–127.89 ($30C_{Ar}$). ^{31}P NMR (CD_3CN, δ): 33.44 (br), 35.98 (br, *J* 7.7 Hz), 42.67 (dt, $^3J_{PP}$ 7.7 Hz, $^3J_{YP}$ 5.4 Hz) ^{89}Y NMR (*via* HMQC, CD_3CN, δ): −1.5. MS, *m*/*z*: 937 (M–NO_3). Analysis: calcd (%) for $C_{42}H_{51}N_5O_{12}P_3Y$: C, 50.46; H, 5.14; N 7.01. Found: C, 50.07; H, 5.26; N, 7.26.

[Y((R_{P1}*,S_{P3}*)-11)$_2(NO_3)$][$(NO_3)_2$ (13). Mp 217–218 °C (dec.). IR (KBr disk): ν_{max}/cm^{-1} 817 (w), 829 (w), 986 (m), 1102 (s), 1173 (s), 1384 (s), 1469 (m). ^{1}H NMR (CD_3CN, δ): 0.63 (d, 12H, $^3J_{HH}$ 6.8 Hz, $4CH_3$), 0.77 (br, 6H, $2CH_3$), 0.81 (d, 24H, $^3J_{HH}$ 6.8 Hz, $8CH_3$), 1.01 (br, 6H, $2CH_3$), 3.32 (dh, 4H, $^3J_{HH}$ 6.8 Hz, 4CH), 3.54 (br, 4H, 4CH), 6.48 (dddd, 2H, $^4J_{HH}$ 0.7 Hz, $^3J_{HH}$ 7.9 Hz, J_{PH} 7.6 Hz, J_{PH} 16.6 Hz, ArH), 6.9 (m, 4H, ArH), 7.0 (m, 6H, ArH), 7.14 (m, 6H, ArH), 7.48 (m, 2H, ArH), 7.65 (ddt, 2H, $^4J_{HH}$ 1.2 Hz, $^3J_{HH}$ 7.6 Hz, J_{PH} 3.2 Hz, ArH). 7.79 (m, 6H, ArH), 7.9 (m, 4H, ArH), 7.98 (ddt, 2H, $^4J_{HH}$ 1.2 Hz, $^3J_{HH}$ 7.6 Hz, J_{PH} 3.2 Hz, ArH), 8.07 (dd, 2H, $^3J_{HH}$ 7.4 Hz, J_{PH} 1.5 Hz, ArH), 8.13 (m, 4H, ArH), 8.38 (dddd, 2H, $^4J_{HH}$ 1.2 Hz, $^3J_{HH}$ 7.7 Hz, J_{PH} 4.3 Hz, J_{PH} 12.1 Hz, ArH), 8.58 (m, 2H, ArH). ^{13}C NMR (CD_3CN, δ): 20.69 (br), 22.42 (d, $^3J_{PC}$ 4.3 Hz), 22.93 (br), 47.34 (br), 47.97 (d, $^2J_{PC}$ 6.2 Hz), 138.25–127.5 ($60C_{Ar}$) ^{31}P NMR (CD_3CN, δ): 34.28 (bt, $^3J_{PP}$ 8.4 Hz), 40.3 (t, $^3J_{PP}$ 8.4 Hz), 42.01 (dt, $^3J_{PP}$ 8.4 Hz, $^3J_{YP}$ 5.6 Hz) ^{89}Y NMR (*via* HMQC and DEPT, CD_3CN, δ): −23.7. MS, *m*/*z*: 1661 (M–NO_3), 1599 (M–$(NO_3)_2$). Analysis: calcd (%) for $C_{84}H_{102}N_7O_{15}P_6Y$: C, 58.50; H, 5.96; N 5.69. Found: C, 57.01; H, 5.28; N, 5.48.[53]

X-ray crystallographic studies of 11–13. A suitable crystal of **11**, **12** and **13** was covered in mineral oil (Aldrich) and mounted onto a glass fiber. The crystal was transferred directly to the cold N_2 stream at 150 K for complex **11** and **13** and 100 K for complex **12** of a Bruker Smart 1000 CCD diffractometer with Mo-Kα (λ = 0.71073 Å). The intensities were measured using the oscillation method. The crystal structures were solved by Patterson methods for **11** and **13** and Charge Flipping method for **12**. The refinement was performed using full-matrix least squares on *F*2. All non-H atoms were anisotropically refined. All H atoms were geometrically placed riding on their parent atoms with isotropic displacement parameters set to 1.2 times the Ueq of the atoms to which they are attached (1.5 for methyl groups).

Crystallographic calculations were carried out by the X-Ray Group, at the University of Oviedo, using the following programs: Bruker Smart[54] for data collection and cell refinement; Bruker Saint[52] for data reduction; DIRDIF-2008[55] for **11**, SUPERFLIP[56] for **12** and SHELX-86[57] for **13** for structure solution; XABS2[58] for refined absorption correction; SHELXL-97[57] for structure refinement and to prepare materials for publication; Mercury[59] and PLATON[60] for the geometrical calculations; ORTEP-3[61] for windows for molecular graphics. Crystal data and structure refinement details for complexes **11–13** are outlined on Table 1.

Crystallographic data (excluding structure factors) for the structures reported in this paper have been deposited in The Cambridge Crystallographic Data Centre no. CCDC:806039 (complex **11**), CCDC:806041 (complex **12**) and CCDC:806040 (complex **13**). These data can be obtained free of charge from the CCDC *via* http://www.ccdc.cam.ac.uk/products/csd/request/

Acknowledgements

Dedicated to the memory of Prof. R. Suau. Financial support by the Ministerio de Ciencia e Innovación (MICINN) (project CTQ2008-117BQU, MAT2006-01997 and 'Factoría de Cristalización' Consolider-Ingenio 2010) and the Ramón y Cajal program (I.F.) is gratefully acknowledged.

Notes and references

1 (*a*) K. L. Nash, R. E. Barrans, R. Chiarizia, M. L. Dietz, M. P. Jensen, P. G. Rickert, B. A. Moyer, P. V. Bonnesen, J. C. Bryan and R. A. Sachleben, *Solvent Extr. Ion Exch.*, 2000, **18**, 605; (*b*) H. Eccles, *Solvent Extr. Ion Exch.*, 2000, **18**, 633; (*c*) W. Li, X. Wang, H. Zhang, S. Meng and D. Li, *J. Chem. Technol. Biotechnol.*, 2007, **82**, 376; (*d*) M. Nilsson and L. Nash, *Solvent Extr. Ion Exch.*, 2007, **25**, 665; (*e*) P. V. Achuthan and C. Janardanan, *J. Radioanal. Nucl. Chem.*, 2011, **287**, 753.
2 (*a*) T. S. Lobana, in *The Chemistry of Organophosphorus Compounds*, ed. F. R. Hartley, Wiley, New York, 1992, vol. 2, ch. 8, pp. 409–566; (*b*) H. H. Dam, D. N. Reinhoudt and W. Verboom, *Chem. Soc. Rev.*, 2007, **36**, 367; (*c*) A. N. Turanov, V. K. Karandashev and V. E. Baulin, *Solvent Extr. Ion Exch.*, 2007, **25**, 165; (*d*) A. N. Turanov, V. K. Karandashev, V. E. Baulin, A. N. Yarkevich and Z. Safronova, *Solvent Extr. Ion Exch.*, 2009, **27**, 551.

3 (*a*) E. P. Horwitz, D. G. Kalina, H. Diamond, G. F. Vandegrift and W. W. Schulz, *Solvent Extr. Ion Exch.*, 1985, **3**, 75; (*b*) J. N. Mathur, M. S. Murali and K. L. Nash, *Solvent Extr. Ion Exch.*, 2001, **19**, 357; (*c*) J. L. Gregg, V. G. Artem and F. V. George, *Solvent Extr. Ion Exch.*, 2010, **28**, 287.

4 (*a*) W. B. Lanham and T. C. Runion, *USAEC Report ORNL-479*, Oak Ridge, Tennessee, 1949; (*b*) D. D. Sood and S. K. Patil, *J. Radioanal. Nucl. Chem.*, 1996, **203**, 547; (*c*) A. P. Paiva and P. Malik, *J. Radioanal. Nucl. Chem.*, 2004, **261**, 485.

5 (*a*) T. M. Ward, I. W. Allcox and G. H. Wahl Jr., *Tetrahedron Lett.*, 1971, **12**, 4421; (*b*) F. Berny, N. Muzet, L. Troxler, A. Dedieu and G. Wipff, *Inorg. Chem.*, 1999, **38**, 1244; (*c*) M. Baaden, F. Berny, C. Boehme, N. Muzet, R. Schurhammer and G. Wipff, *J. Alloys Compd.*, 2000, **303–304**, 104; (*d*) C. Boehme and G. Wipff, *Inorg. Chem.*, 2002, **41**, 727; (*e*) B. Coupez, C. Boehme and G. Wipff, *Phys. Chem. Chem. Phys.*, 2002, **4**, 5716.

6 For recent references see: (*a*) M. Bosson, W. Levason, T. Patel, M. C. Popham and M. Webster, *Polyhedron*, 2001, **20**, 2055; (*b*) J. Fawcett, A. W. G. Platt and D. R. Russell, *Polyhedron*, 2002, **21**, 287; (*c*) J.-C. Berthet, M. Nierlich and M. Ephritikhine, *Polyhedron*, 2003, **22**, 3475; (*d*) M. J. Glazier, W. Levason, M. L. Matthews, P. L. Thornton and M. Webster, *Inorg. Chim. Acta*, 2004, **357**, 1083; (*e*) A. P. Hunter, A. M. J. Lees and A. W. G. Platt, *Polyhedron*, 2007, **26**, 4865; (*f*) S. Mishra, *Coord. Chem. Rev.*, 2008, **252**, 1996; (*g*) A. Bowden, A. W. G. Platt, K. Singh and R. Townsend, *Inorg. Chim. Acta*, 2010, **363**, 243.

7 For recent references see: (*a*) A. M. J. Lees and A. W. G. Platt, *Inorg. Chem.*, 2003, **42**, 4673; (*b*) A. M. J. Lees and A. W. G. Platt, *Polyhedron*, 2005, **24**, 427; (*c*) Z. Spichal, M. Necas and J. Pinkas, *Inorg. Chem.*, 2005, **44**, 5673; (*d*) K. Matloka, A. K. Sah, M. W. Peters, P. Srinivasan, A. V. Gelis, M. Regalbuto and M. J. Scott, *Inorg. Chem.*, 2007, **46**, 10549; (*e*) Z. Spichal, V. Petricek, J. Pinkas and M. Necas, *Polyhedron*, 2008, **27**, 283; (*f*) M. A. Subhan, Y. Hasegawa, T. Suzuki, S. Kaizaki and Y. Shozo, *Inorg. Chim. Acta*, 2009, **362**, 136.

8 (*a*) B. M. Rapko, E. N. Duesler, P. H. Smith, R. T. Paine and R. R. Ryan, *Inorg. Chem.*, 1993, **32**, 2164; (*b*) E. M. Bond, E. N. Duesler, R. T. Paine and H. Nöth, *Polyhedron*, 2000, **19**, 2135; (*c*) X. Gan, R. T. Paine, E. N. Duesler and H. Nöth, *Dalton Trans.*, 2003, 153; (*d*) X. Gan, B. M. Rapko, E. N. Duesler, I. Binyamin, R. T. Paine and B. P. Hay, *Polyhedron*, 2005, **24**, 469; (*e*) S. Pailloux, C. E. Shirima, A. D. Ray, E. N. Duesler, R. T. Paine, J. R. Klaehn, M. E. McIlwain and B P. Hay, *Inorg. Chem.*, 2009, **48**, 3104.

9 (*a*) R. T. Paine, Y.-C. Tan and X.-M. Gan, *Inorg. Chem.*, 2001, **40**, 7009; (*b*) A. G. Matveeva, E. I. Matrosov, Z. A. Starikova, G. V. Bodrin, S. V. Matseev, P. V. Petrovskii and E. E. Nifant'ev, *Russ. Chem. Bull.*, 2005, **54**, 2519; (*c*) A. G. Matveeva, E. I. Matrosov, Z. A. Starikova, G. V. Bodrin, S. V. Matseev and E. E. Nifant'ev, *Russ. J. Inorg. Chem.*, 2006, **51**, 253.

10 K. Miyata, Y. Hasegawa, Y. Kuramochi, T. Nakagawa, T. Yokoo and T. Kawai, *Eur. J. Inorg. Chem.*, 2009, 4777.

11 (*a*) G. Vicentini and P. O. Dunstan, *J. Inorg. Nucl. Chem.*, 1971, **33**, 1749; (*b*) G. Vicentini and J. C. Prado, *J. Inorg. Nucl. Chem.*, 1972, **34**, 1309; (*c*) L. B. Zinner and G. Vicentini, *Inorg. Chim. Acta*, 1975, **15**, 235; (*d*) L. R. F. Carvalho, G. Vicentini and K. Zinner, *J. Inorg. Nucl. Chem.*, 1981, **43**, 1088; (*e*) J. R. Matos, L. B. Zinner, K. Zinner, G. Vicentini and P. O. Dunstan, *Thermochim. Acta*, 1993, **219**, 173.

12 (*a*) G. Vicentini and L. S. P. Braga, *J. Inorg. Nucl. Chem.*, 1971, **33**, 2959; (*b*) G. Vicentini and P. O. Dunstan, *J. Inorg. Nucl. Chem.*, 1972, **34**, 1303; (*c*) G. Vicentini, L. B. Zinner and L. Rothschild, *Inorg. Chim. Acta*, 1974, **9**, 213; (*d*) G. Vicentini and L. C. Machado, *J. Inorg. Nucl. Chem.*, 1981, **43**, 1676.

13 L. B. Zinner, G. Vicentini and L. Rothschild, *J. Inorg. Nucl. Chem.*, 1974, **36**, 2499.

14 A. R. de Aquino, G. Bombieri, P. C. Isolani, G. Vicentini and J. Zucherman-Schpector, *Inorg. Chim. Acta*, 2000, **306**, 101.

15 E. E. Castellano, G. Oliva and J. Zuckerman-Schpector, *Inorg. Chim. Acta*, 1985, **109**, 33.

16 Phosphine oxide complexes: (*a*) M. J. McGeary, P. S. Coan, K. Folting, W. E. Streib and K. G. Caulton, *Inorg. Chem.*, 1991, **30**, 1723; (*b*) W. A. Herrmann, R. Anwander, V. Dufaud and W. Scherer, *Angew. Chem., Int. Ed. Engl.*, 1994, **33**, 1285; (*c*) L. Deakin, W. Levason, M. Popham, G. Reid and M. Webster, *J. Chem. Soc., Dalton Trans.*, 2000, 2439; (*d*) W. Levason, B. Patel, M. C. Popham, G. Reid and M. Webster, *Polyhedron*, 2001, **20**, 2711; (*e*) Y.-C. Tan, X.-M Gan, J. L. Stanchfield, E. N. Duesler and R. T. Paine, *Inorg. Chem.*, 2001, **40**, 2910; (*f*) A. Tutaβ, M. Goldner, H. Hückstädt, U. Cornelissen and H. Homborg, *Z. Anorg. Allg. Chem.*, 2001, **627**, 2323; (*g*) N. J. Hill, W. Levason, M. C. Popham, G. Reid and M. Webster, *Polyhedron*, 2002, **21**, 445.

17 L. Fuks and M. Majdan, *Miner. Proces. Extr. Metall. Rev.*, 2000, **21**, 25.

18 I. Fernández, P. Oña-Burgos, J. M. Oliva and F. López-Ortiz, *J. Am. Chem. Soc.*, 2010, **132**, 5193.

19 (*a*) I. Fernández, P. Oña-Burgos, G. Ruiz-Gomez, C. Bled, S. García-Granda and F. López-Ortiz, *Synlett*, 2007, 611; (*b*) P. Oña-Burgos, I. Fernández, L. Roces, L. Torre-Fernández, S. García-Granda and F. López-Ortiz, *Organometallics*, 2009, **28**, 1739.

20 C. Popovici, P. Oña-Burgos, I. Fernández, L. Roces, S. García-Granda, M. J. Iglesias and F. López-Ortiz, *Org. Lett.*, 2010, **12**, 428.

21 (*a*) P. Caravan, T. Hedlund, S. Liu, S. Sjobergand and C. Orvig, *J. Am. Chem. Soc.*, 1995, **117**, 11230; (*b*) A. Fujiwara, Y. Nakano, T. Yaita and K. Okuno, *J. Alloys Compd.*, 2008, **456**, 429.

22 M. F. Davis, W. Levason, G. Reid and M. Webster, *Polyhedron*, 2006, **25**, 930.

23 M. A. Bennett, C. J. Cobley, A. D. Rae, E. Wenger and A. C Willis, *Organometallics*, 2000, **19**, 1522.

24 F. Bigoli, P. Deplano, M. L. Mercuri, M. A. Pellinghelli and E. F. Trogu, *Phosphorus, Sulfur Silicon Relat. Elem.*, 1992, **70**, 145.

25 $Ph_2P(O)NMe_2$: (*a*) M. ul-Haque and C. N. Caughlan, *J. Chem. Soc., Perkin Trans. 2*, 1976, 1101; $Ph_2P(O)NMe(CH_2)_2Ph$: (*b*) F. Cameron and F. D. Duncanson, *Acta Crystallogr., Sect. B: Struct. Crystallogr. Cryst. Chem.*, 1981, **37**, 1604; $Ph_2P(O)N(CH_2)_2$: (*c*) B. Davidowitz, T. A. Modro and M. L. Niven, *Phosphorus Sulfur Relat. Elem.*, 1985, **22**, 255.

26 (*a*) I. Fernández, A. Forcén-Acebal, S. García-Granda and F. López-Ortiz, *J. Org. Chem.*, 2003, **68**, 4472; (*b*) H. De Bod, D. B. G. Williams, A. Roodt and A. Muller, *Acta Crystallogr., Sect. E: Struct. Rep. Online*, 2004, **60**, o1241.

27 A P–O bond distance of 1.506(2) Å has been reported for an *ortho*-stannyl *N*,*N*-diisopropylphosphinic amide showing intramolecular oxygen–tin interaction. See reference 19b.

28 F. H. Allen, O. Kennard, D. G. Watson, L. Brammer, A. G. Orpen and R. Taylor, *J. Chem. Soc., Perkin Trans. 2*, 1987, S1.

29 (*a*) D. R. Cousins and F. A. Hart, *J. Inorg. Nucl. Chem.*, 1967, **29**, 1745; (*b*) D. R. Cousins and F. A. Hart, *J. Inorg. Nucl. Chem.*, 1968, **30**, 3009.

30 The free ligand shows two P═O stretching bands at 1227 and 1209 cm^{-1}, whereas only a broad band is observed for complex **12**.

31 (*a*) M. G. B. Drew, *Coord. Chem. Rev.*, 1977, **24**, 179; (*b*) R. M. Hartshorn, E. Hey-Hawkins, R. Kalio and G. J. Leigh, *Pure Appl. Chem.*, 2007, **79**, 1779.

32 X.-M. Gan, E. N. Duesler and R. T. Paine, *Inorg. Chem.*, 2001, **40**, 4420.

33 W. Levason, E. H. Newman and M. Webster, *Polyhedron*, 2000, **19**, 2697.

34 An analogous arrangement is found in europium complexes of tridentate triphosphine trioxides. See reference 10.

35 L. Troxler, A. Dedieu, F. Hutschka and G. Wipff, *THEOCHEM*, 1998, **431**, 151.

36 J. L. Hoard and J. V. Silverton, *Inorg. Chem.*, 1963, **2**, 235.

37 E. M. Bond, X. Gan, J. R. FitzPatrick and R. T. Paine, *J. Alloys Compd.*, 1998, **271–273**, 172.

38 Although the coupling of the isopropyl protons with ^{31}P could not be resolved, its existence was evidenced by the narrowing of the corresponding signals when the ^{1}H NMR spectrum was measured under ^{31}P decoupling. Additionally, this coupling allowed us to establish the connectivity within the $P(O)N^{i}Pr_2$ frameworks through the correlations observed in the ^{1}H, ^{31}P-HMQC spectrum for the methyl protons.

39 (*a*) D. Rehder, in *Transition Metal Nuclear Magnetic Resonance*, ed. P. S. Pregosin, Elsevier, Amsterdam, 1991, pp. 1–58; (*b*) R. E. White and T. P. Hanusa, *Organometallics*, 2006, **25**, 5621.

40 (*a*) J. Kronenbitter and A. Schwenk, *J. Magn. Reson.*, 1977, **25**, 147; (*b*) R. M. Adam, G. V. Fazakerley and D. G. Reid, *J. Magn. Reson.*, 1979, **33**, 655; (*c*) G. C. levy, P. L. Rinaldi and J. T. Bailey, *J. Magn. Reson.*, 1980, **40**, 167; (*d*) J. Epinger, M. Spiegler, W. Hieringer, W. A. Herrmann and R. Anwander, *J. Am. Chem. Soc.*, 2000, **122**, 3080.

41 D. L. Reger, J. A. Lindeman and L. Lebioda, *Inorg. Chem.*, 1988, **27**, 1890.

42 K. C. Hultzsch, P. Voth, K. Beckerle, T. P. Spaniol and J. Okuda, *Organometallics*, 2000, **19**, 228.

43 (*a*) M. Zimmermann, N. A. Frøystein, A. Fischbach, P. Sirsch, H. M. Dietrich, K. W. Törnroos, E. Herdtweck and R. Anwander, *Chem.–Eur. J.*, 2007, **13**, 8784; (*b*) M. Zimmermann, F. Estler, E. Herdtweck, K. W. Törnroos and R. Anwander, *Organometallics*, 2007, **26**, 6029; (*c*) M. Zimmermann, D. Rauschmaier, K. Eichele, K. W. Törnroos and R. Anwander, *Chem. Commun.*, 2010, **46**, 5346.

44 I. Fernández, V. Yañez-Rodríguez and F. López Ortiz, *Dalton Trans.*, 2011, **40**, 2425.

45 The spectrum obtained using a delay of 83.3 ms corresponding to the experimental $^{2}J_{YP}$ of *ca.* 6 Hz does not show the correlation between P3 and ^{89}Y due to the rapid transverse relaxation of the relatively broad P3 signal.

46 (*a*) P. Stilbs, *Prog. Nucl. Magn. Reson. Spectrosc.*, 1987, **19**, 1; (*b*) C. S. Johnson Jr., *Prog. Nucl. Magn. Reson. Spectrosc.*, 1999, **34**, 203; (*c*) F. Stallmach and P. Galvosas, *Annu. Rep. NMR Spectrosc.*, 2007, **61**, 51.

47 (*a*) Y. Cohen, L. Avram and L. Frish, *Angew. Chem., Int. Ed.*, 2005, **44**, 520; (*b*) T. Brand, E. J. Cabrita and S. Berger, *Prog. Nucl. Magn. Reson. Spectrosc.*, 2005, **46**, 159; (*c*) P. S. Pregosin, P. G. A. Kumar and I. Fernandez, *Chem. Rev.*, 2005, **105**, 2977; (*d*) A. Macchioni, G. Ciancaleoni, C. Zuccaccia and D. Zuccaccia, *Chem. Soc. Rev.*, 2008, **37**, 479; (*e*) G. Bellachioma, G. Ciancaleoni, C. Zuccaccia, D. Zuccaccia and A. Macchioni, *Coord. Chem. Rev.*, 2008, **252**, 2224.

48 Satisfactory results were obtained by using saturated solutions due to the very poor solubility of **11** in acetonitrile.

49 (*a*) K. G. Spears and L. E. Cramer, *Chem. Phys.*, 1978, **30**, 1; (*b*) P. Schurtenberger and M. E. Newman, in *Environmental Particles*, ed. J. Buffle and H. P. van Leeuwen, Lewis, Boca Raton, FL, 1993, vol. 2, pp. 37; (*c*) K. W. Mattison, U. Nobbmann and D. Dolak, *Am. Biotech. Lab.*, 2001, **19**, 66.

50 A. B. Pangborn, M. A. Giardello, R. H. Grubbs, R. K. Rosen and F. J. Timmers, *Organometallics*, 1996, **15**, 1518.

51 B. Burns, N. P. King, H. Tye, J. R. Studley, M. Gamble and M. Wills, *J. Chem. Soc., Perkin Trans. 1*, 1998, 1027.

52 P. Stilbs, *Prog. Nucl. Magn. Reson. Spectrosc.*, 1987, **19**, 1.

53 The relatively large deviations of the elemental analysis found with respect to the calculated values might be due to the presence of small amounts of yttrium hydroxide that could not be eliminated through four purification cycles.

54 *Area-Detector Software Package*, SMART & SAINT, Bruker, 2007.

55 P. T. Beurskens, G. Beurskens, R. de Gelder, S. Garcia-Granda, R. O. Gould and J. M. M. Smits, *The DIRDIF2008 program system*, Crystallography Laboratory, University of Nijmegen, The Netherlands, 2008.

56 L. Palatinus and G. Chapuis, *J. Appl. Crystallogr.*, 2007, **40**, 786.

57 G. M. Sheldrick, *Acta Crystallogr., Sect. A: Found. Crystallogr.*, 2007, **64**, 112.

58 S. Parkin, B. Moezzi and H. J. Hope, *J. Appl. Crystallogr.*, 1995, **28**, 53.

59 C. F. Macrae, P. R. Edgington, P. McCabe, E. Pidcock, G. P. Shields, R. Taylor, M. Towler and J. J. van de Streek, *J. Appl. Crystallogr.*, 2006, **39**, 453.

60 (*a*) A. L. Spek, *Acta Crystallogr. A*, 1990, **A46**, C34; (*b*) *PLATON, A Multipurpose Crystallographic Tool*, Utrecht University, Utrecht, The Netherlands, A. L. Spek, 1998.

61 L. J. Farrugia, *J. Appl. Crystallogr.*, 1997, **30**, 565.